Journal of Biomolecular NMR, **25:** 91–103, 2003.
KLUWER/ESCOM

Determination of the torsion angles of alanine and glycine residues of model compounds of spider silk $(AGG)_{10}$ using solid-state NMR methods

Jun Ashida[a,b], Kosuke Ohgo[a], Kohei Komatsu[a], Ayumi Kubota[a] & Tetsuo Asakura[a,*]
[a]*Department of Biotechnology, Tokyo University of Agriculture and Technology, Koganei, Tokyo 184-8588, Japan*
[b]*Varian Technologies Japan Ltd., Minato, Tokyo 108-0023, Japan*

Received 26 July 2002; Accepted 18 November 2002

Key words: ^{13}C chemical shift contour plot, Flagelliform silk, Poly(Ala-Gly-Gly), REDOR, Spider dragline silk, 2D spin-diffusion NMR under off magic angle spinning

Abstract

Spiders synthesize several kinds of silk fibers. In the primary structure of spider silk, one of the major ampullate (dragline, frame) silks, spidroin 1, and flagelliform silk (core fibers of adhesive spiral), there are common repeated X-Gly-Gly (X = Ala, Leu, Pro, Tyr, Glu, and Arg) sequences, which are considered to be related to the elastic character of these fibers. In this paper, two dimensional spin diffusion solid-state NMR under off magic angle spinning (OMAS), ^{13}C chemical shift contour plots, and Rotational Echo DOuble Resonance (REDOR) were applied to determine the torsion angles of one Ala and two kinds of Gly residues in the Ala-Gly-Gly sequence of ^{13}C=O isotope-labeled $(Ala\text{-}Gly\text{-}Gly)_{10}$. The torsion angles were determined to be $(\phi, \psi) = (-90°, 150°)$ within an experimental error of $\pm 10°$ for each residue. This conformation is characterized as 3_1 helix which is in agreement with the structure proposed from the X-ray powder diffraction pattern of poly(Ala-Gly-Gly). The 3_1 helix of $(Ala\text{-}Gly\text{-}Gly)_{10}$ does not change by formic acid treatment although $(Ala\text{-}Gly)_{15}$ easily changes from the silk I conformation (the structure of *Bombyx mori* silk fibroin before spinning in the solid state) to silk II conformation (the structure of the silk fiber after spinning) by such treatment. Thus, the 3_1 helix conformation of $(Ala\text{-}Gly\text{-}Gly)_{10}$ is considered very stable. Furthermore, the torsion angles of the 16th Leu residue of $(Leu\text{-}Gly\text{-}Gly)_{10}$ were also determined as $(\phi, \psi) = (-90°, 150°)$ and this peptide is also considered to take 3_1 helix conformation.

Introduction

The silk fibers produced by spiders or silkworms are the nature's most highly engineered structural materials with combinations of strength and toughness not found in today's man-made materials (O'Brien et al., 1998). The dragline silk fibers produced by spiders have been focus of numerous recent investigations because they have a tensile strength that is comparable to Kevlar (4×10^9 Nm^{-2}) coupled with a reasonable elasticity (35%), and therefore they are known as an extremely strong fiber (Gosline et al., 1999). The major ampullate dragline silk from *Nephila clavipes* has been studied in detail (O'Brien et al., 1998; Warner et al., 1999; Winkler and Kaplan, 2000). The primary structure of the dragline silk is quite different from the silk fiber from silkworm, *Bombyx mori* which is well known as excellent textile material. The dragline silk contains major ampullate spider silk 1 (MaSp1) and major ampullate spider silk 2 (MaSp2) (Hinman et al., 2000). The primary structure of MaSp1 has been reported as the repetition of two unique motifs – poly-Ala regions and Gly-rich regions (Lewis, 1992) as shown in Figure 1a. Poly-Ala regions contain 5 to 6 Ala residues and Gly-rich regions contains 18 to 40 residues. The structure of the poly-Ala region in the dragline silk has been characterized as β-sheet, and this region is considered to be crystalline which contributes to the high strength of the dragline silk (Parkhe et al., 1997; Bram et al., 1997; Simmons

*To whom correspondence should be addressed. E-mail: asakura@cc.tuat.ac.jp

(a) Dragline silk (MaSp1)

QGAGAAAAAAGGAGQGGYGGLGGQGAGQGGYGGLGGQGAGQGAGAAAAAA
AGGAGQGGYGGLGSQGAGRGGQGAGAAAAAAGGAGQGGYGGLGSQGAGRG
GLGGQGAGAAAAAAAGGAGQGGYGGLGNQGAGRGGQGAAAAAAGGAGQGG
YGGLGSQGAGRGGLGGQAGAAAAAAGGAGQGGYGGLGGQGAGQGGYGGLG
SQGAGRGGLGGQGAGAAAAAAAGGAGQGGLGGQGAGQGAGASAAAAGGAG
QGGYGGLGSQGAGRGGEGAGAAAAAAGGAGQGGYGGLGGQGAGQGGYGGL
GSQGAGRGGLGGQGAGAAAAAGQGAGAAAAAAGGAGQGGYGGLGSQGAGR
GGLGGQGAGAVAAAAAGGAGQGGYGGLGSQGAGRGGQGAGAAAAAAGGAG
QRGYGGLGNQGAGRGGLGGQGAGAAAAAAAGGAGQGGYGGLGNQGAGRGG
QGAAAAAGGAGQGGYGGLGSQGAGRGGQGAGAAAAAAVGAGQEGIRGQGA
GQGGYGGLGSQGSGRGGLGGQGAGAAAAAAGGAGQGGLGGQGAGQGAGAA
AAAAGGVRQGGYGGLGSQGAGRGGQGAGAAAAAAGGAGQGGYGGLGGQGV
GRGGLGGQGAGAAAAGGAGQGGYGGVGSGASAASAAAASRLSS

(b) Flagelliform silk

VGPGGSGPGGYGPGGSGPGGYGPGGAGPGGYGPGGSGPGGYGPGGSGPGG
YGPGGSGPGGYGPGGSGPGGYGSGGAGPGGYGPGGSGPGGYGPGGSGPGG
YGPGGTGPGGTGPGGSGPGGYGPGGSGPGGSGPGGSGPGGYGPSGSGPGG
YGPSGSGPGGYGPGGSGPGGYGPGGSGAGGTGPGGAGGAGGAGGSGGAGG
SGGAGGSGGAGGSGGVGGSGGTTITEDLDITIDGADGPITISEELTISGA
GGSGPGGAGPGVGPGGSGPGGVGPGVSGPGGVGPGGSGPGGVGSGGSGPG
GVGPGGYGPGGSGSGGVGPGGYGPGGSGGFYGGPGGSEGPYGPSGPYGSG
GGYGPGGAGGPYGPGSPGGAYGPGSPGGAYYPSSRVPDMVNGIMSAMQGS
GFNYQMFGNMLSQYSSGSGTCNPNNVNVLMDALLAALHCLSNHGSSSFAP
SPTPAAMSAYSN

Figure 1. The primary structures of the *Nephila clavipes* spider silk; (a) the major ampullate spider silk (MaSp1) and (b) Flagelliform silk. The X-Gly-Gly units are underlined.

et al., 1994, 1996; Gosline et al., 1999). On the other hand, the structural analysis of the Gly-rich region is relatively difficult because there is a variety of the Gly-containing sequences which produce several possibilities about the local structure such as random coil, β-sheet and 3_1 helix including the conformational equilibrium. In Figure 1a, it is noted that there are characteristic repeated sequences such as X-Gly-Gly (where X=Ala, Leu, Pro, Tyr, Glu, and Arg). Therefore the presence of a 3_1 helix in the Gly-rich region is thought likely because Poly(Ala-Gly-Gly) or Poly(Pro-Gly-Gly) takes on a 3_1 helical conformation (Lotz and Keith, 1971; Brack and Spach, 1968; Traub, 1969). Actually, the Gly-rich region in the dragline silk from the spider *Nephila madagascariensis* was reported to adopt a 3_1 helix from the 2D spin-diffusion powder spectrum of [1-^{13}C]Gly dragline silk fiber (Kummerlen et al., 1996). The X-Gly-Gly sequences can be found even more frequently in the core fibers of the adhesive capture spiral in flagelliform silk as shown in Figure 1b (Hayashi and Lewis, 1998).

In our previous papers, we could use several solid state NMR techniques, namely, 2D spin-diffusion solid-state NMR under OMAS and REDOR together with the quantitative analysis of the ^{13}C chemical shifts with the conformation-dependent chemical shift contour plots, to determine the torsion angles of the backbone structure of the alternating copolypeptide

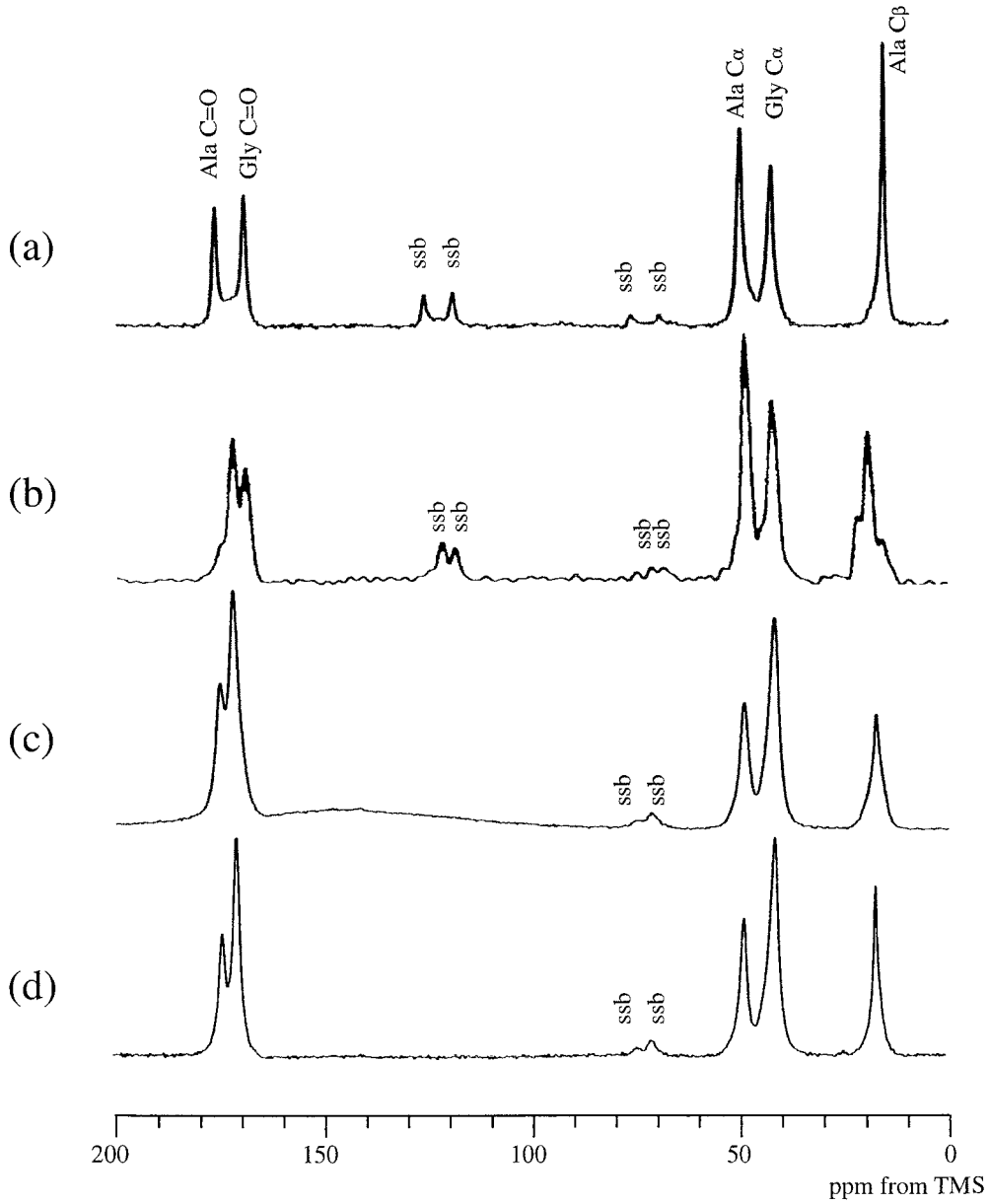

Figure 2. ^{13}C CP/MAS spectra of dried solid derived from $(Ala\text{-}Gly)_{15}$ dissolved in 9M LiBr and dialyzed against water (a), $(Ala\text{-}Gly)_{15}$ dissolved in formic acid (b), $(Ala\text{-}Gly\text{-}Gly)_{10}$ dissolved in 9M LiBr and dialyzed against water (c) and $(Ala\text{-}Gly\text{-}Gly)_{10}$ dissolved in formic acid (d). ssb means spinning sideband.

$(Ala\text{-}Gly)_{15}$ as the model peptide of *B. mori* silk fibroins in the silk I (the solid state structure before spinning) form. The advantages of the combination of these solid state NMR techniques for the structural analysis of these peptides including the advantage of using 2D spin-diffusion NMR under OMAS have been described in our previous papers (Asakura et al., 2001a, 2002; Ashida et al., 2002).

In this paper, the determination of the detailed structure of $(Ala\text{-}Gly\text{-}Gly)_{10}$ was performed as a model of 13 repeats XGG in flagelliform silk. The torsion angles of the Ala and Gly residues of ^{13}C isotope-labeled $(Ala\text{-}Gly\text{-}Gly)_{10}$ were determined with ^{13}C two-dimensional spin-diffusion solid-state NMR under OMAS, REDOR (Gullion and Schaefer, 1989) and the ^{13}C chemical shifts together with the chemi-

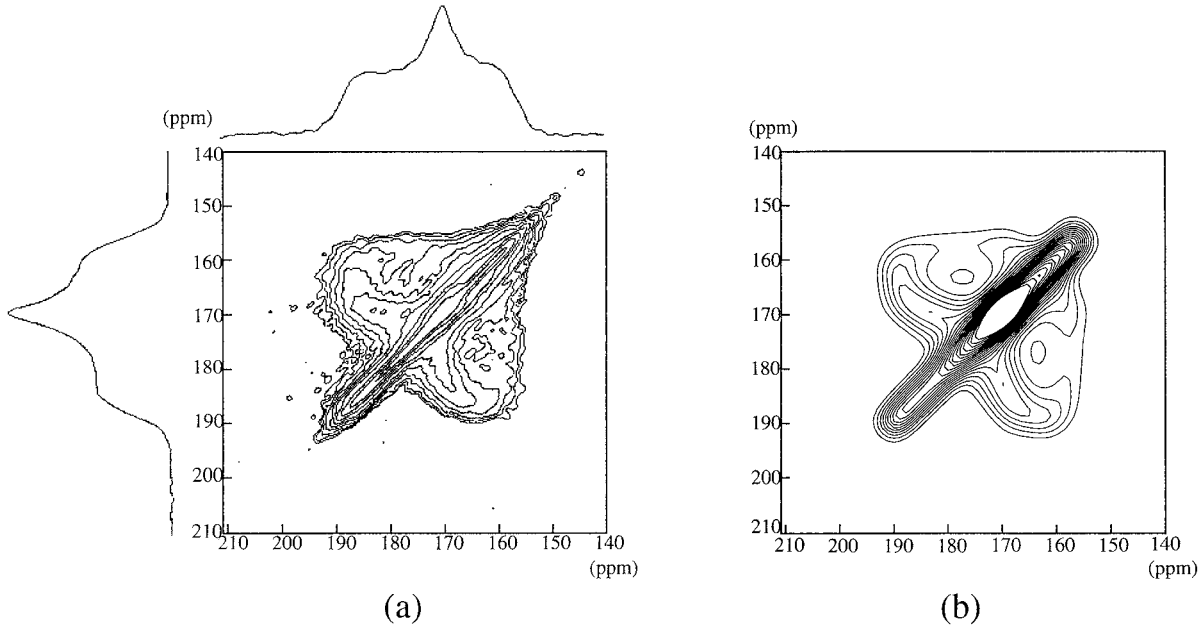

Figure 3. 2D spin-diffusion spectrum of $(AGG)_4A[1\text{-}^{13}C]G\ [1\text{-}^{13}C]G(AGG)_5$ (a) and the simulated spectrum (b) when the (ϕ, ψ) angles of the 15th Gly residue are ($-90°$, $150°$).

cal shift contour plots (Iwadate et al., 1999; Asakura et al., 1999a). The determination of the torsion angles of the 16th Leu residue was also performed with ^{13}C two-dimensional spin-diffusion solid-state NMR for $(Leu\text{-}Gly\text{-}Gly)_{10}$. Reversely, the typical pattern of ^{13}C spin diffusion NMR and ^{13}C chemical shift data for 3_1-helix was reported and will be able to use as the indication of 3_1-helix structure.

Materials and methods

The several ^{13}C and/or ^{15}N selectively isotope labeled Ala and Gly containing copolypeptides, $(AGG)_{10}$, $(AGG)_4A[1\text{-}^{13}C]G[1\text{-}^{13}C]G(AGG)_5$, $(AGG)_4[1\text{-}^{13}C]A\text{-}[1\text{-}^{13}C]GG(AGG)_5$, $(AGG)_4AG[1\text{-}^{13}C]G[1\text{-}^{13}C]A\text{-}GG(AGG)_4$, and $(AGG)_4AG[1\text{-}^{13}C]G\text{-}A[^{15}N]GG(A\text{-}GG)_4$ were synthesized by the solid phase method (Pioneer Peptide Synthesizer Co. Ltd.) for 2D spin-diffusion NMR and REDOR experiments. All these samples were dissolved in 9M LiBr aqueous solution and dialyzed against 3M LiBr aqueous solution for 3 h. Then it was dialyzed against distilled water for 3 days. The precipitated samples were collected and dried before NMR measurements. $(AGG)_{10}$ was also dissolved in formic acid and dried. ^{13}C selectively isotope labeled Leu and Gly containing copolypeptide $(LGG)_4LG[1\text{-}^{13}C]G[1\text{-}^{13}C]LGG(LGG)_4$ was also synthesized by the solid phase method for 2D spin-diffusion NMR. This sample was dissolved in trifluoroacetic acid and dried.

The 2D spin-diffusion solid-state NMR spectra under OMAS condition were obtained with Varian UNITY*INOVA* 400 MHz NMR spectrometer and 7 mmϕ AutoMAS HX probe at off magic angle condition (63°) and sample spinning speed of 6 kHz ($\pm$5 Hz) at room temperature. The mixing time of 2 s was optimized for spin-diffusion between intramolecular specific carbons of selectively isotope-labeled Ala and/or Gly residues; spin-diffusion between inter-molecular carbons was suppressed. The recycle delay (2 s) was carefully determined from the 1D OMAS spectra under several recycle times for each sample. The contact time was set to 2 ms using the Variable-Amplitude CP (VACP) technique (Peersen et al., 1993). An 81 kHz rf field strength was used for ^1H decoupling during evolution and acquisition periods. The $\pi/2$ pulse length for ^1H and ^{13}C were 3.2 and 3.6 μs, respectively. The angle θ between static magnetic field and sample spinning axes was determined by the measurements of scaled ^{13}C chemical shielding anisotropy (CSA) spectra of β-quinol methanol under OMAS. The CSA of the benzene carbon of β-quinol methanol is 176 ppm and therefore the scaling factor and the angle θ were easily calculated from the

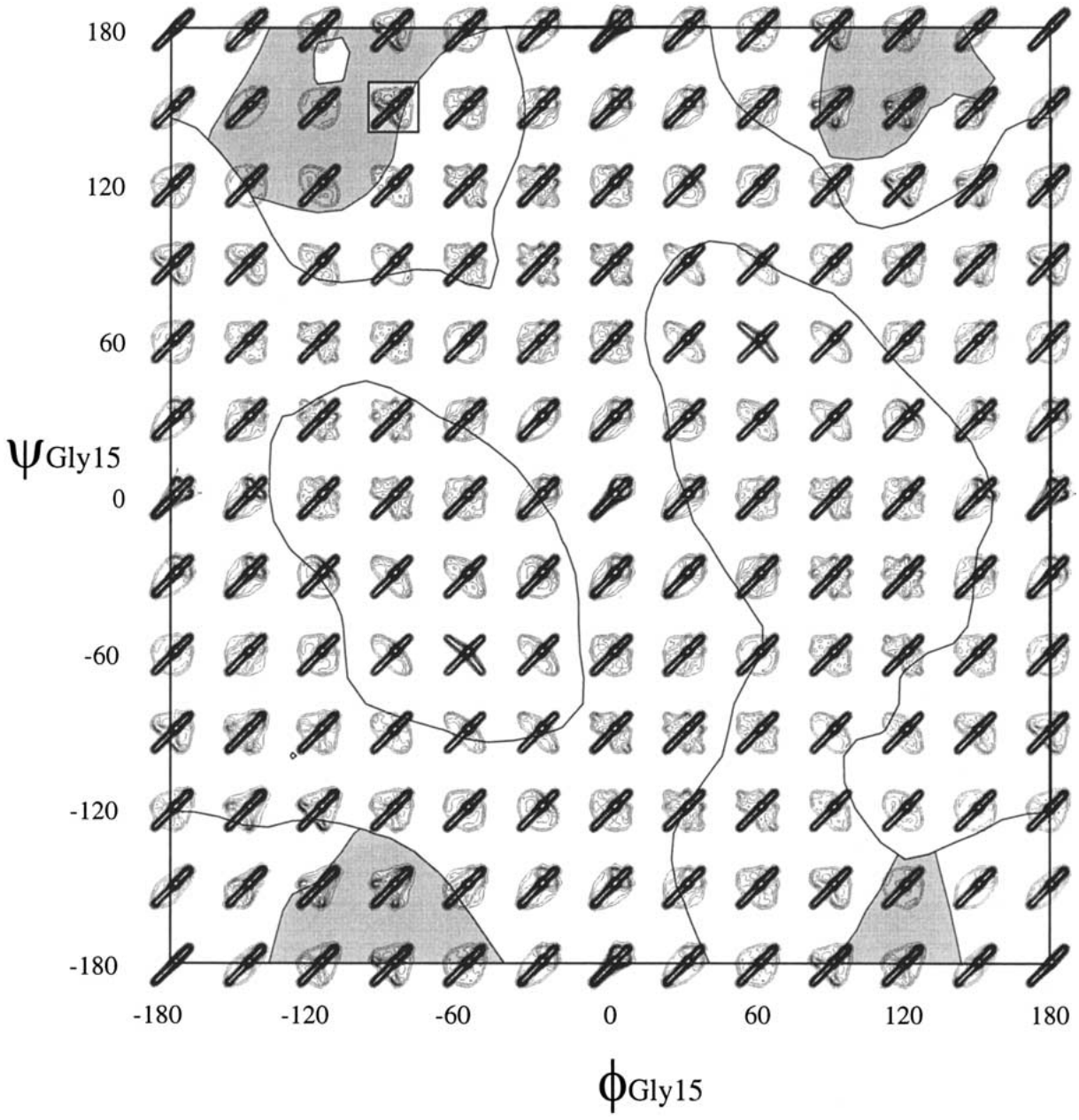

Figure 4. Ramachandran map of the calculated 2D spin-diffusion spectra as a function of (ϕ, ψ) of Gly for each 30°. Chemical shift values in the region ($-180° < \phi < 180°$, $-180° < \psi < 180°$) in which the density function is greater than 1, are surrounded by the solid lines. The area which satisfies the observed Gly C^{α} chemical shift of 41.6 ± 0.5 ppm was shown as a shadow region, where random coil chemical shift of Gly C^{α} carbon is 42.7 ppm (Asakura et al., 1999a). The torsion angles (ϕ, ψ) = ($-90°$,150°) gave a good agreement between the calculated and observed 2D spin-diffusion spectra as shown in Figure 3.

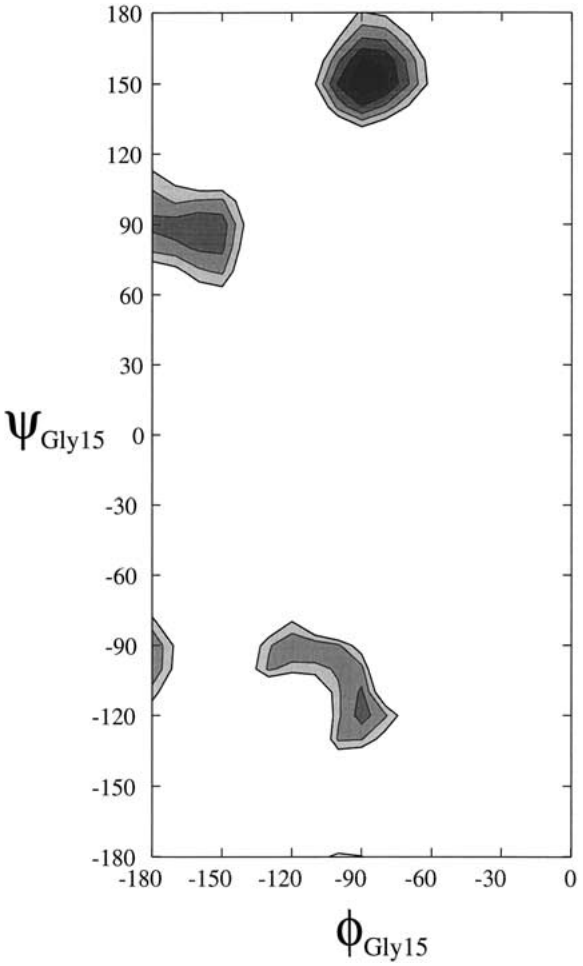

Figure 5. Contour plot of χ^2 deviation for 2D spin diffusion spectrum of $(AGG)_4A[1\text{-}^{13}C]$ $G[1\text{-}^{13}C]G(AGG)_5$. Here $\chi^2(\phi, \psi = \frac{1}{\sigma^2}\Sigma_{i=1}^{N}\ [E_i - S_i(\phi, \psi)]^2$ where σ is the root-mean-squared noise in the experimental spectrum, N is the number of intensities analyzed, Ei are the experimental intensities, Si(ϕ, ψ) are the calculated intensities.

scaled CSA powder pattern under OMAS. The chemical shift tensors of the carbonyl carbons of $[1\text{-}^{13}C]$ Ala and Gly residues of the samples were determined from the spinning sideband pattern of slow spinning CP/MAS spectra obtained using a Chemagnetics Infinity 400 MHz NMR spectrometer (Herzfeld and Berger, 1980).

A calculation program, developed in our laboratory, was used to simulate the 2D spin-diffusion NMR spectra (Levitt et al., 1990; Asakura et al., 2001a; Ashida et al., 1990, 2002). The relative orientation between the chemical shift tensors of the carbonyl carbons and the molecular frame used in this work is the following (Oas et al., 1987; Teng and Cross, 1989; Demura et al., 1998; Asakura et al., 1998); σ_{33} is perpendicular to the O – C′ – N plane, σ_{22} is parallel to the C=O bond although σ_{22} deviates by about 10°, and σ_{11} is in the O – C′ – N plane, and perpendicular to both σ_{22} and σ_{33}. For 2D spin-diffusion NMR simulation, the calculations were performed using a grid of 10° for ϕ and ψ values. An OCTANE (Silicon Graphics Inc.) workstation was used for the calculation of the theoretical spectra. The χ^2 value was introduced to demonstrate the difference between the experimental and calculated spectra quantitatively. The definition of the χ^2 was

$$\chi^2(\phi, \psi) = \frac{1}{\sigma^2}\sum_{i=1}^{N}\left[E_i - S_i(\phi, \psi)\right]^2,$$

where σ is the root-mean-squared noise in the experimental spectrum, N is the number of intensities analyzed, Ei are the experimental intensities, Si(ϕ, ψ) are the calculated intensities.

The REDOR NMR experiment was performed using the Chemagnetics Infinity 400 MHz spectrometer and Varian/Chemagnetics 4 mmϕ T3 HXY probe. The sample spinning speed was set to be 6666 Hz. The contact time was set to 1.0 ms with the rf field strength of 62.5 kHz. 100 kHz rf field strength was used for ^{1}H decoupling. The π pulse length for ^{13}C and ^{15}N were 8.0 and 9.0 μs, respectively. The recycle delay was set to 3.0 s. Phases of ^{15}N π pulses were cycled according to the XY-4 scheme to minimize the off-resonance and pulse error effects (Gullion et al., 1990; Gullion and Schaefer, 1991). REDOR evolution times ranged up to 18 ms (120 rotor cycles).

The torsion angles which satisfy the observed distance between the carbonyl carbon of the 15th Gly and the nitrogen of the 17th Gly were calculated by taking into account the experimental error and shown in the Ramachandran map of the 16th Ala residue.

Results

^{13}C CP/MAS *spectra of* (Ala-Gly-Gly)$_{10}$

Figure 2a shows ^{13}C CP/MAS spectrum of $(Ala\text{-}Gly)_{15}$ in the silk I form reported previously (Asakura et al., 2001a, b). This form was prepared by dissolving $(Ala\text{-}Gly)_{15}$ in 9M LiBr and then dialyzed against water. With solid state NMR technique such as two dimensional spin diffusion solid-state NMR under OMAS, REDOR, and conformation-dependent ^{13}C chemical shift contour plots, the structure of silk I was characterized as β-turn type II form. On the

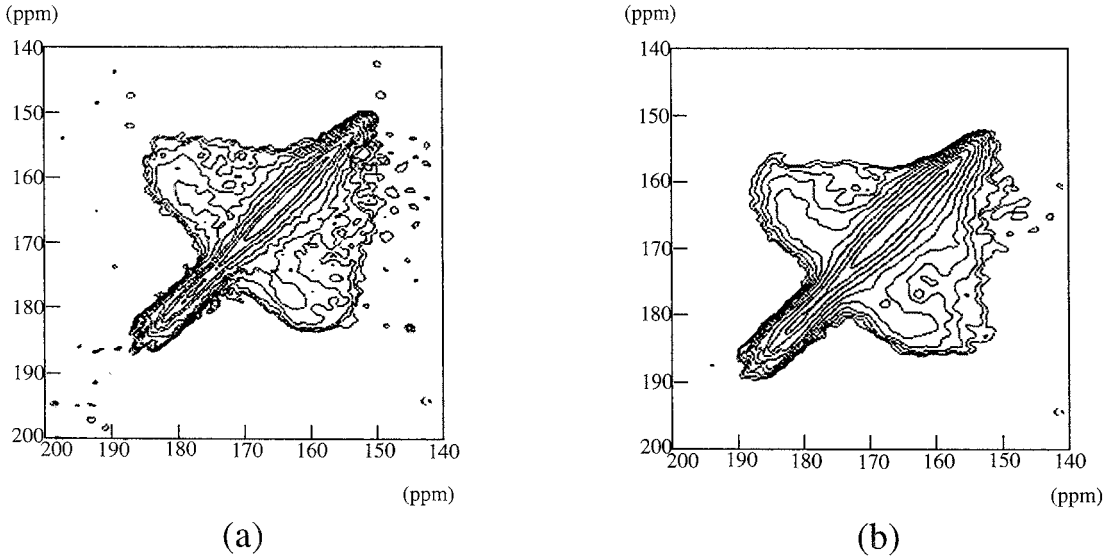

Figure 6. 2D spin-diffusion spectra of $(AGG)_4AG[1\text{-}^{13}C]G[1\text{-}^{13}C]AGG(AGG)_4$ (a) and $(AGG)_4[1\text{-}^{13}C]A\ [1\text{-}^{13}C]GG(AGG)_5$ (b).

other hand, the silk I form of $(Ala\text{-}Gly)_{15}$ changes to silk II form (the solid state structure after spinning) after dissolving the sample in formic acid and then dried. The silk II structure is heterogeneous as judged from the asymmetric peak of the Ala C^{β} carbon (Figure 2b). Detailed structural analysis has been reported by us (Asakura et al., 2002). It consists of 27% distorted β-turn which corresponds to a broad peak at around 16.5 ppm, which is characterized by a large distribution in torsion angles around an averaged conformation of a type II β-turn. The other two components of the asymmetric Ala C^{β} peak with chemical shifts of 19.6 and 21.9 ppm were assigned to anti-parallel β-sheet structure. Since the Ala C^{β} methyl groups are located outside of the protein backbone, the occurrence of two peaks suggests that there may exist differences in the mode of side-chain packing, while the same backbone torsion angles are maintained. In conclusion, the peak at 21.9 ppm with relative intensity of 27% was assigned to the Ala methyl groups which were oriented in the same direction between the adjacent β-sheets. On the other hand, the highest peak at 19.6 ppm with relative intensity of 46% was assigned to the Ala methyl groups which were oriented in the opposite direction between the adjacent β-sheets.

The ^{13}C CP/MAS NMR spectrum of $(Ala\text{-}Gly\text{-}Gly)_{10}$ which was prepared after dissolving $(Ala\text{-}Gly\text{-}Gly)_{10}$ in 9M LiBr and dialyzed against water is shown in Figure 2c. The method for the sample preparation

Table 1. ^{13}C CP/MAS NMR chemical shifts of $(Ala\text{-}Gly)_{15}$ and $(Ala\text{-}Gly\text{-}Gly)_{10}$ (ppm from TMS)

Sample	Ala			Gly	
	C^{β}	C^{α}	C=0	C^{α}	C=0
$(AG)_{15}$[a]	16.5	50.7	176.8	43.2	169.9
$(AG)_{15}$[b]	16.7 19.6 22.2	48.7	171.8	42.4	169.1
$(AGG)_{10}$[a]	17.4	48.9	174.6	41.6	171.3
$(AGG)_{10}$[b]	17.3	48.8	174.6	41.4	171.2

[a]The sample was dissolved in 9M LiBr and dialyzed against 3M LiBr for 3 h. Then it was dialyzed against distilled water from 3 days and dried.
[b]The sample was dissolved in formic acid and dried.

is the same as that for $(Ala\text{-}Gly)_{15}$ in the silk I form. The Ala C^{β} peak is slightly broader than the Ala C^{β} peak of $(Ala\text{-}Gly)_{15}$ in the silk I form (Figure 2a), but a single peak. Thus, the structure of $(Ala\text{-}Gly\text{-}Gly)_{10}$ seems homogeneous. All the ^{13}C chemical shifts of Gly and Ala residues of $(Ala\text{-}Gly\text{-}Gly)_{10}$ listed in Table 1 are quite different from those of $(Ala\text{-}Gly)_{15}$ in silk I or silk II forms, indicating that the structure of $(Ala\text{-}Gly\text{-}Gly)_{10}$ is different from β-turn or β-sheet structures. Figure 2d shows the ^{13}C CP/MAS NMR spectrum of $(Ala\text{-}Gly\text{-}Gly)_{10}$ which was prepared after dissolving $(Ala\text{-}Gly\text{-}Gly)_{10}$ in formic acid and dried. This treatment of the $(Ala\text{-}Gly)_{15}$ induces the structural change from silk I to silk II as mentioned above. However, Figure 2d is basically the same as Figure 2c although the spectrum becomes slightly sharper. Thus,

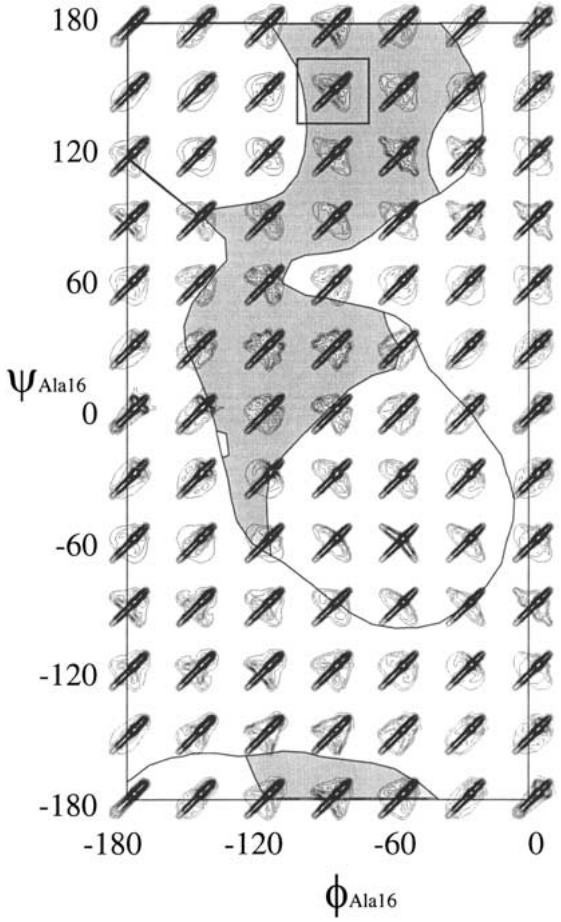

Figure 7. Ramachandran map of the calculated 2D spin-diffusion spectra as a function of (ϕ, ψ) of Ala for each 30°. The shadow region indicates the area where the combined chemical shift error is less than 1 ppm. The details are described in the text. The torsion angles (ϕ, ψ) = (−90°,150°) gave a good agreement between the calculated and observed 2D spin-diffusion spectra.

the structural change does not occur essentially by the formic acid treatment for $(Ala\text{-}Gly\text{-}Gly)_{10}$. This indicates that the structure of $(Ala\text{-}Gly\text{-}Gly)_{10}$ is very stable. The detailed structure will be determined in the following sections.

2D spin diffusion spectrum of
$(AGG)_4A[1\text{-}^{13}C]\text{-}G[1\text{-}^{13}C]G(AGG)_5$

The 2D solid-state NMR spectroscopy is very effective to determine the torsion angles of the specified residue of the backbone chain of $[1\text{-}^{13}C]$ double-labeled peptides (Tycko, 2001; van Beek et al., 2000; Asakura et al., 2001a; Ashida et al., 2002). Figure 3 shows 2D spin-diffusion solid-state NMR spectrum (only the carbonyl carbon region was expanded) of $(AGG)_4A[1\text{-}^{13}C]G[1\text{-}^{13}C]G(AGG)_5$ together with the spectrum calculated by assuming the torsion angles of the 15th Gly residue as (ϕ, ψ) = (−90°, 150°). The calculated spectra for each 30° as a function of (ϕ, ψ) of the 15th Gly residue are shown in Figure 4. For the calculation, it is necessary to obtain the principal values of the chemical shift tensors of the carbonyl carbon atom of Gly residue. Thus, by observing the sample under slow MAS, the principal values of the chemical shift for Gly carbonyl carbon atom were determined. The calculated spectral patterns change largely depending on (ϕ, ψ), but the patterns are the same between (ϕ, ψ) and ($-\phi$, $-\psi$) because of the reorientation between the molecular frame, and the principal axis frame of the chemical shift tensor of Gly carbonyl carbon. In order to further narrow down the area in the Ramachandran map, the C^α chemical shift (41.6 ± 0.5 ppm) of Gly residue was used (Iwadate et al., 1999). The area with enough data points to give reliable chemical shift predictions for the C^α carbon chemical shifts of Gly residues, in which the density function is greater than 1, are surrounded by the solid lines. The area predicted from the chemical shift of 41.6 ± 0.5 ppm for the Gly C^α carbon are shadowed. Moreover, the quantitative analysis of the difference between calculated and observed spin diffusion NMR spectra was performed. The difference $\chi^2(\phi, \psi)$ was calculated and shown in Figure 5. Thus, the torsion angles were determined to be (ϕ, ψ) = (−90°, 150°) for the 15th Gly residue. The experimental error was ±10°. The character of the experimental spectrum was well reproduced.

2D spin diffusion spectrum of
$(AGG)_4AG[1\text{-}^{13}C]\text{-}G[1\text{-}^{13}C]AGG(AGG)_4$

The observed 2D spin-diffusion solid-state NMR spectrum (only the carbonyl carbon region was expanded) of $(AGG)_4AG[1\text{-}^{13}C]G[1\text{-}^{13}C]AGG(AGG)_4$ is shown in Figure 6a. The spectrum is also similar to that of 15th Gly residue mentioned above although this pattern gives the torsion angles of the 16th Ala residue of $(Ala\text{-}Gly\text{-}Gly)_{10}$. This suggests that the torsion angles are also similar to the angles of 15th Gly residues. Figure 7 shows the calculated spectra for each 30° as a function of (ϕ, ψ) of the 16th Ala residue. The calculated spectral patterns change largely depending on (ϕ, ψ) which is similar to the case of 15th Gly residue as shown in Figure 4. In order to further narrow down the area in the Ramachandran map, the C^α (48.9 ± 0.5 ppm) and C^β (17.4 ± 0.5 ppm) chemical shifts of

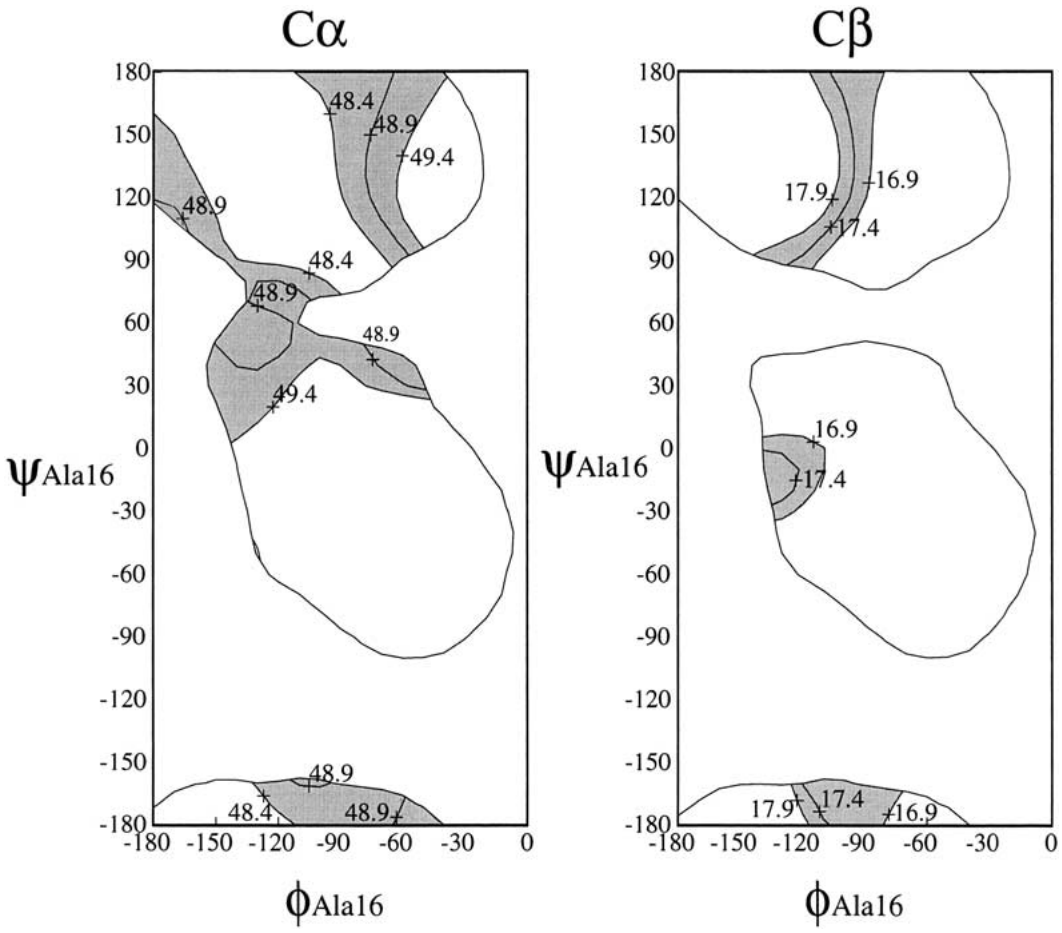

Figure 8. The chemical shift contour maps of the conformation-dependent chemical shifts (in ppm) of C^{α} and C^{β} carbons of Ala residues. Chemical shift values in the region ($-180° < \phi < 0°$, $-180° < \psi < 180°$) in which the density function is greater than 1, are surrounded by the solid lines. The area which satisfies the observed C^{α} (48.9 ± 0.5 ppm) and C^{β} (17.4 ± 0.5 ppm) chemical shifts of Ala residue was shown as a shadow region. Random coil chemical shifts are 50.0 ppm for Ala Ca carbon and 16.6 ppm for Ala C^{β} carbon (Asakura et al., 1999a).

Ala residue were used (Iwadate et al., 1999). The area with enough data points to give reliable chemical shift predictions for both the C^{α} and C^{β} chemical shifts of Ala residues in Ramachandran map ($-180° < \phi < 0°$, $-180° < \psi < 180°$) in which the density function is greater than 1, are surrounded by the solid lines in Figure 8. The area predicted from the isotropic chemical shifts of Ala C^{α} and C^{β} carbons are shadowed. Then, it is necessary to find out the areas which satisfy observed both C^{α} and C^{β} chemical shifts of Ala residue. For the purpose, we calculated the root-mean-square difference between the observed C^{α} and C^{β} chemical shifts for the different structure and the estimated shifts from the chemical shift contour maps of Ala residues and then selected the area indicated by the lines as a combined chemical shift error of less than 1 ppm in Figure 7 as shadowed region. By checking the observed 2D spin-diffusion spectrum carefully, the torsion angles were determined to be $(\phi, \psi) = (-90°, 150°)$ for the 16th Ala residue. The experimental error was $\pm 10°$.

2D spin diffusion spectrum of $(AGG)_4[1\text{-}^{13}C]A[1\text{-}^{13}C]GG(AGG)_5$

The 2D spin-diffusion solid-state NMR spectrum (only the carbonyl carbon region was expanded) $(AGG)_4[1\text{-}^{13}C]A[1\text{-}^{13}C]GG(AGG)_5$ is shown in Figure 6b. The spectral pattern is similar to Figures 3a and 6a. The calculated spectra (Figure 7) for each 30° as a function of (ϕ, ψ) of the 16th Ala residue as mentioned before, are also used as the calculated spectra as a function of $(-\psi, -\phi)$ of the 14th Gly residue

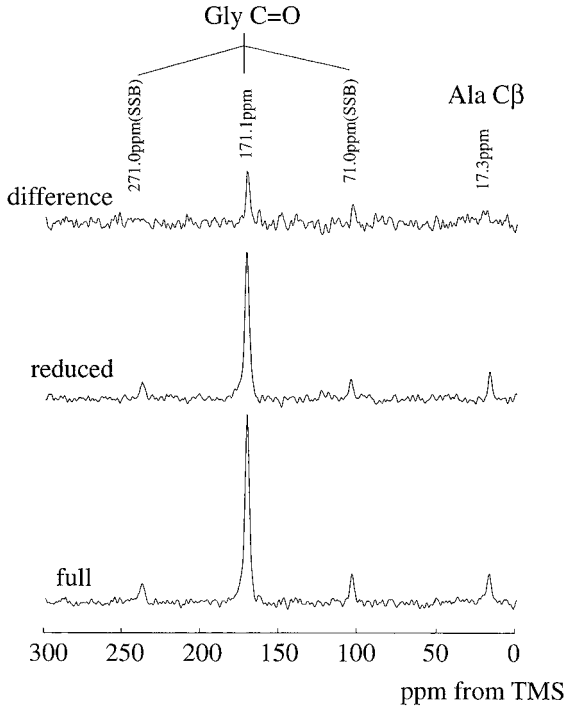

Figure 9. ^{13}C detected-REDOR spectra for $(AGG)_4AG[1\text{-}^{13}C]GA[^{15}N]GG(AGG)_4$ with a spinning speed of 6666 Hz and 80 rotor cycles. Bottom: The full spectrum (rotational spin echo). Middle: The reduced spectrum (^{15}N π pulses applied). Top: The difference spectrum (the reduced spectrum was subtracted from the full spectrum).

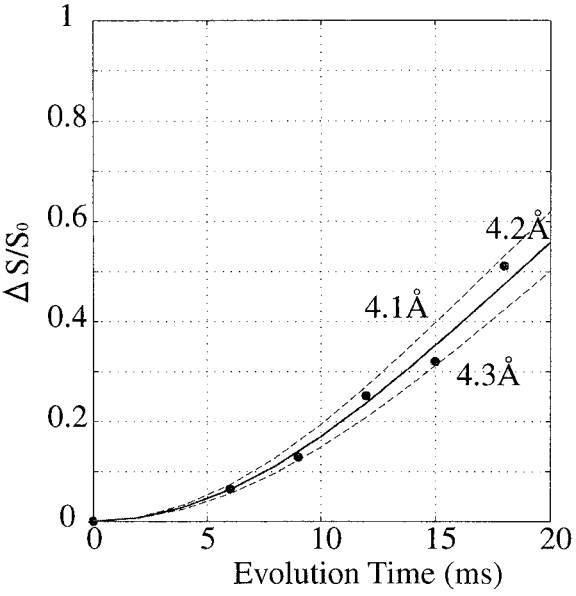

Figure 10. Experimental REDOR plots $\Delta S/S_0$ $(=1-S/S_0)$ for $(AGG)_4AG[1\text{-}^{13}C]GA[^{15}N]GG(AGG)_4$. ΔS and S_0 are the REDOR amplitudes and full echo amplitudes, respectively. Solid and dashed lines show the calculated dephasing curves corresponding to the designated distances.

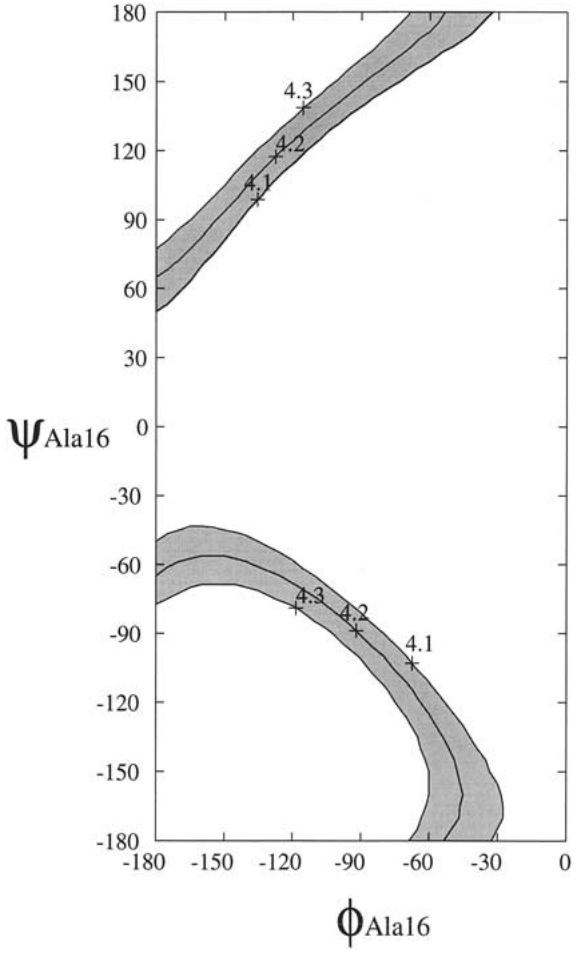

Figure 11. The conformational map for the torsion angles (ϕ, ψ) of the 15th Ala residue which satisfies the ^{13}C-^{15}N distance for $(AGG)_4AG[1\text{-}^{13}C]GA[^{15}N]GG(AGG)_4$ of 4.2 ± 0.1 Å determined by REDOR experiment.

because of the reorientation between the molecular frame, and the principal axis frame of the chemical shift tensor of Ala and Gly carbonyl carbons. Thus, by checking the observed 2D spin-diffusion spectrum carefully, the torsion angles were determined to be $(\phi, \psi) = (-90°, 150°)$ for the 14th Gly residue as well as the 15th Gly and 16th Ala residues.

REDOR *spectrum of* $(AGG)_4AG[1\text{-}^{13}C]GA[^{15}N]GG\text{-}(AGG)\text{-}_4$

In order to confirm the torsion angles determined in the previous sections, REDOR experiment was performed. Figure 9 shows the ^{13}C REDOR full-echo, reduced, and difference spectra of $(AGG)_4AG[1\text{-}^{13}C]GA[^{15}N]GG(AGG)_4$. The experimental ^{13}C RE-

DOR plot, $\Delta S/S_0$ vs evolution time, for $(AGG)_4AG[1\text{-}^{13}C]GA[^{15}N]GG(AGG)_4$ is shown in Figure 10. Solid and dashed lines show calculated dephasing curves corresponding to the designated distances. By comparing the REDOR experimental plot with the calculated dephasing curves, the ^{13}C-^{15}N distance for $(AGG)_4AG[1\text{-}^{13}C]GA[^{15}N]GG(AGG)_4$ was determined as 4.2 Å within an error of ±0.1 Å. This distance between the isotope labeled ^{13}C and ^{15}N atoms is in good agreement with the predicted value of 4.1 Å when the torsion angles, ϕ and ψ of the Ala and Gly residues are (−90°, 150°). The torsion angles which satisfy the observed distance between the carbonyl carbon of the 15th Gly and the nitrogen of the 17th Gly were calculated by taking into account the experimental error, 4.2 ± 0.1 Å, and shown in the Ramachandran map of the 16th Ala residue (Figure 1). Thus, the error in (ϕ, ψ) estimated from the error in the REDOR experiments was about ± 10°.

2D spin diffusion spectrum of $(LGG)_4LG[1\text{-}^{13}C]\text{-}G[1\text{-}^{13}C]LGG(LGG)_4$

As shown in Figure 1, it is noted that there are characteristic repeated sequences such as X-Gly-Gly (where X = Ala, Leu, Pro, Tyr, Glu, and Arg) in spider silk. We tried to determine the torsion angles of Ala and Gly residues of $(Ala\text{-}Gly\text{-}Gly)_{10}$ in the previous sections. In order to check whether or not these angles are also applicable to the other sequence in the spider silk, 2D spin diffusion spectrum was observed for $(Leu\text{-}Gly\text{-}Gly)_{10}$. The 2D spin-diffusion solid-state NMR spectrum (only the carbonyl carbon region was expanded) of $(LGG)_4LG[1\text{-}^{13}C]G[1\text{-}^{13}C]LGG(LGG)_4$ is shown in Figure 12. The spectral pattern gives the torsion angles of the 16th Leu residue of $(Leu\text{-}Gly\text{-}Gly)_{10}$. The 2D spin diffusion NMR spectrum of $(LGG)_4LG[1\text{-}^{13}C]G[1\text{-}^{13}C]LGG(LGG)_4$ is very similar to that of $(AGG)_4AG[1\text{-}^{13}C]G[1\text{-}^{13}C]AGG(AGG)_4$ (Figure 6(a)). Therefore, it is likely that the structure of $(Leu\text{-}Gly\text{-}Gly)_{10}$ is similar to the structure of $(Ala\text{-}Gly\text{-}Gly)_{10}$.

Discussion

Lotz and Keith (1971) prepared the structure of poly(Ala-Gly-Gly) in the form II by dialyzing 1% solution of the polymer in 60% aqueous LiBr against similar solutions of LiBr which were diluted progressively with water. The sample precipitates when the concentration of LiBr in the mother liquor has reached 30 to 40%. The crystal was analyzed with X-ray powder diffraction. In the preparation of our $(Ala\text{-}Gly\text{-}Gly)_{10}$ sample before solid state NMR observation, the sample was dissolved in 9MLiBr aqueous solution and dialyzed against 3M LiBr aqueous solution for 3 h. Then it was dialyzed against distilled water for 3 days. Thus, the structure is considered the same between these two samples. Brack and Spach (1968) showed that the crystal of poly(Ala-Gly-Gly) in the form II is a 3_1-helical structure with a hydrated form of the polymer incorporating one molecule of water per tripeptide, the water being firmly bound since it may be removed under vacuum only if the crystals are heated. After dehydration, the crystals give X-ray diffraction patterns with fewer reflections and with the longest spacing reduced from 11.0 to 10.1 Å. Lotz and Keith indexed all observed reflections from the poly(Ala-Gly-Gly) in the form II in terms of a monoclinic cell having a = 11.0 Å, b = 4.8 Å, c (chain axis) = 9.45 Å, β = 90°. The crystal structure was proposed to be 3_1 helix with the torsion angles were (ϕ, ψ) (−80°, 150°), which is slightly different from those in poly-Gly II due to the small increase in chain-axis repeat from 9.30 to 9.45 Å. This proposed structure is basically the same as the 3_1 helix reported for poly(Pro-Gly-Gly) (Traub, 1969). In our study, the torsion angles of one Ala residue and two Gly residues in the central Ala-Gly-Gly sequence of (Ala-

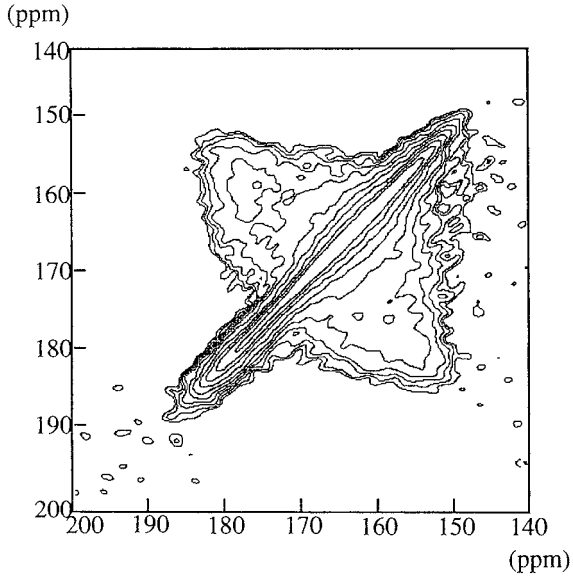

Figure 12. 2D spin-diffusion spectrum of $(LGG)_4LG[1\text{-}^{13}C]G[1\text{-}^{13}C]LGG(AGG)_4$.

Gly-Gly)$_{10}$ were determined as (ϕ, ψ) = ($-90°$, $150°$) with the experimental error of $\pm 10°$. Thus the structure proposed by us is essentially the same structure reported by Lotz and Keith for Poly(Ala-Gly-Gly). The ^{13}C chemical shifts of the Ala and Gly residues determined clearly in this paper are quite different from those of β-sheet, β-turn type II (silk I), and α-helix, which gives a comparison with the 3_1 helical conformation (Table 1) (Saito et al., 1984). Especially, it should be noted that the Gly C^{α} chemical shift is a good indicator of the 3_1 helical conformation. However, the Gly chemical shifts, especially the carbonyl carbon chemical shift change significantly by changing the primary structure and therefore it is necessary to use that chemical shift carefully for discussion of the secondary structure (Ando et al., 1988; Asakura et al., 1984, 1985, 1988).

A structural change of (Ala-Gly-Gly)$_{10}$ does not occur upon treatment with formic acid although (Ala-Gly)$_{15}$ easily undergoes the structural change from silk I to silk II by such treatment. Thus, the 3_1 helix structure of (Ala-Gly-Gly)$_{10}$ is considered very stable. The 2D spin diffusion NMR spectrum of (LGG)$_4$LG[1-^{13}C]G[1-^{13}C]LGG(LGG)$_4$ is very similar to that of (AGG)$_4$AG[1-^{13}C]G[1-^{13}C]AGG(AGG)$_4$ as shown in Figure 12. Therefore, the 3_1 helix structure is still maintained even if a Leu residue is used instead of the Ala residue of (Ala-Gly-Gly)$_{10}$. As mentioned above, poly(Pro-Gly-Gly) also takes on a 3_1 helical conformation (Taube, 1969). This means there are no severe steric conflicts in the intra- and intermolecular arrangements of these peptide chains in the 3_1-helical form. As shown in Figure 1, it is noted that there are characteristic repeated sequences such as X-Gly-Gly(where X = Ala, Leu, Pro, Tyr, Glu, and Arg). However, we speculate that the 3_1 conformation will be maintained even if Ala or Leu are changed to other amino acids in the repeated X-Gly-Gly sequence.

In spider dragline silk fiber, major ampullate spidroin 1, there is repetition of two unique motifs – poly-Ala regions and Gly-rich regions (Lewis, 1992). Thus, the structure of the Gly-rich region might be influenced by the presence of the β-sheet structure of poly-Ala region. The structure of silk fibroin fiber from a wild silkworm, *Samia cynthia ricini,* whose amino acid sequence is similar to the spider (major ampullate) silk, (i.e., repeats of poly-Ala and Gly-rich regions,) was determined with solid state NMR previously (Asakura et al., 1999b). The ^{15}N and ^{13}C labelings for the dominant amino acids, Ala and Gly residues of *S. c. ricini* silk fibroin were performed by oral administration of ^{15}N Ala, [1-^{13}C]Ala, ^{15}N Gly or [1-^{13}C]Gly to the 5th instar larvae of the silkworm, *S. c. ricini*. The silk fibroin stored in the silkgland was stretched by about 10 times the original length of the sample and the blocks of the oriented fibers were prepared for ^{15}N and ^{13}C solid state NMR observation. All of the oriented spectra of [^{15}N]Gly and [1-^{13}C]Gly silk fibroin fiber blocks (Demura et al., 1998) are similar to the spectra of [^{15}N]Ala and [1-^{13}C]Ala silk fibroin fiber blocks, respectively, and the fraction of the oriented components was determined as 75% for Ala site and 65% for Gly site (Asakura et al.,1999b). The conformation of the oriented components is concluded as β-sheet and the un-oriented components which give powder pattern spectra is considered mainly random coil.

There is controversy about the conformation of the Gly residue in Gly-rich sequences of spider silk which, in turn, is similar to the Gly-rich sequences of *S. c. ricini* silk fibroin. Judging from the similar primary structure including Gly residues between *S. c. ricini* silk and spider silk, the sequences in spider silk might be mainly β-sheet. Actually, Thiel et al. (1994) showed recently the presence of β-sheet structure including the fact that Gly residues are required in order to interpret large crystal size predicted from careful X-ray diffraction analysis. Fukushima (1998a, b) prepared the seven repetitive polypeptides matching the Gly-rich sequence of spider dragline silk by a recombinant DNA technique. The FT-IR data of the samples prepared as a cast film from formic acid showed a β-sheet structure. Because of the length of the poly-Ala region is different between two silk fibroins (the number of Ala residue is 12–13 for *S. c. ricini* silk, but 5–6 for spider dragline silk), the ability to incorporate the Gly-rich region into the β-sheet structure might be stronger for the former silk. Actually, the Gly-rich region in the dragline silk from the spider *Nephila madagascariensis* has been reported to adopt a 3_1 helix from the 2D spin-diffusion powder spectrum of [1-^{13}C]Gly dragline silk fiber (Kummerlen et al., 1996). The primary structure of the Gly-rich region in the spider dragline silk is quite different from the Gly-rich region in the spider fragelliform silk, and more complex than the simple repeated sequence, X-Gly-Gly as shown in Figure 1a. Thus we will try to prepare the peptide with more complicated sequences shown in Figure 1a including the poly-Ala region. The combination of 2D spin diffusion NMR under OMAS, REDOR and use of chemical shift contour maps when two adequate pairs are isotope-labeled has

a high potential for determining the torsion angles in the repeated sequence.

Conclusions

By using two-dimensional spin-diffusion solid-state NMR under OMAS and REDOR together with ^{13}C conformation-dependent chemical shift contour plots, the torsion angles ϕ and ψ of one Ala and two kinds of Gly residues in Ala-Gly-Gly sequence of (Ala-Gly-Gly)$_{10}$ were determined as ($-90°$, 150^o). The experimental error was $\pm 10°$ for each torsion angle. From these torsion angles, the structure of (Ala-Gly-Gly)$_{10}$ was determined as 3_1-helix. The 3_1-helix structure of (Leu-Gly-Gly)$_{10}$ was also determined by using two-dimensional spin-diffusion solid-state NMR.

Acknowledgement

TA acknowledges supports from Bio-oriented Technology Research Advancement Institution.

References

Ando, S., Ando, I., Shoji, A. and Ozaki, T. (1988) *J. Am. Chem. Soc.*, **110**, 3380–3386.

Asakura, T. and Murakami, T. (1985) *Macromolecules*, **18**, 2614–2619.

Asakura, T., Ashida, J., Yamane, T., Kameda, T., Nakazawa,Y., Ohgo, K. and Komatsu, K. (2001a) *J. Mol. Biol.*, **306**, 291–305.

Asakura, T., Yamane, T., Nakazawa, Y., Kameda, T. and Ando, K. (2001b) *Biopolymers*, **58**, 521–525.

Asakura, T., Iwadate, M., Demura, M. and Williamson, M.P. (1999a) *Int. J. Biol. Macromol.*, **24**, 167–171.

Asakura, T., Ito, T., Okudaira, M. and Kameda, T. (1999b) *Macromolecules*, **32**, 4940–4946.

Asakura, T., Kashiba, H. and Yoshimizu, H. (1988) *Macromolecules*, **21**, 644–648.

Asakura, T., Watanabe, Y. and Ito, T. (1984) *Macromolecules*, **17**, 2421–2426.

Asakura, T., Yao, J., Yamane, T.,Umemura, K. and Ulrich, A.S. (2002) *J. Am. Chem. Soc.*, **124**, 8794–8795.

Asakura, T., Yamazaki, Y., Koo, W.S. and Demura, M. (1998) *J. Mol. Struct.*, **446**, 179–190.

Ashida, J., Kuwahara, D., Uegaki, T. and Terao, T. (1990) In *Proceedings of the NMR Conference, Kyoto*, pp. 245–246.

Ashida, J., Ohgo K. and Asakura T. (2002) *J. Phys. Chem.*, **B106**, 9434–9439.

Brack, A. and Spach, G. (1968) In *9^{th} European Symposium on Peptides*, Orsay, 45, North Holland Pubishing Co. Amsterdam.

Bram, A., Branden, C.I., Craig, C., Snigireva, I. and Riekel, C. (1997) *J. Appl. Cryst.*, **30**, 390–392.

Demura, M., Minami, M., Asakura, T. and Cross, T.A. (1998) *J. Am. Chem. Soc.*, **120**, 1300–1308.

Fukushima,Y. (1998a) *Biopolymers*, **45**, 269–279.

Fukushima,Y. (1998b) *Chem. Lett.*, 939–940.

Gosline, J.M., Guerette, P.A., Ortlepp, C.S. and Savage, K.N. (1999) *J. Exp. Biol.*, **202**, 3295–3303.

Gullion, T. and Schaefer, J. (1989) *Adv. Magn. Reson.*, **13**, 57–83.

Gullion, T. and Schaefer, J. (1991) *J. Magn. Reson.*, **92**, 439–442.

Gullion, T., Baker, D.B. and Schaefer, J. (1990) *J. Magn. Reson.*, **89**, 479–484.

Hayashi, C.Y. and Lewis, R.V. (1998) *J. Mol. Biol.*, **275**, 773–784.

Herzfeld, J. and Berger, A.E. (1980) *J. Chem. Phys*, **73**, 6021–6030.

Hinman, M.B., Jones, J.A. and Lewis, R.V. (2000) *Tibtech September*, **18**, 374–379.

Iwadate, M., Asakura, T. and Williamson, M.P. (1999) *J. Biomol. NMR*, **13**, 199–211.

Kummerlen, J., van Beek, J.D., Vollrath, F. and Meier, B.H. (1996) *Macromolecules*, **29**, 2920–2928.

Levitt, M.H., Raleigh, D.P., Creuzet, F. and Griffin, R.G. (1990) *J. Chem. Phys*., **92**, 6347–6364.

Lewis, R.V. (1992) *Accounts Chem. Res.*, **25**, 392–397.

Lotz, B. and Keith, H.D. (1971) *J. Mol. Biol.*, **61**, 195–200.

Oas, T.G., Hartzell, C.J., Dahlquist, F.W. and Drobny, G.P. (1987) *J. Am. Chem. Soc*., **109**, 5962–5966.

O'Brien, J.P., Fahnestock, S.R., Termonia, Y. and Gardner, K.H. (1998) *Adv. Mater.*, **10**, 1185–1195.

Parkhe, A.D., Seeley, S.K., Gardener, K., Thompson, L. and Lewis, R.B. (1997) *J. Mol. Recogn.*, **10**, 1–6.

Peersen, O., Wu, X., Kustanovich, I. and Smith, S.O. (1993) *J. Magn. Reson. Ser.*, **A104**, 334–339.

Saito, H., Tabeta, R., Shoji, A., Ozaki, T., Ando, I. and Miyata, T. (1984) *Biopolymers*, **23**, 2279–2297.

Simmons, A.H., Michal, C.A. and Jelinski, J.W. (1996) *Science*, **271**, 84–87.

Simmons, A.H., Ray, E. and Jelinski, J.W. (1994) *Macromolecules*, **27**, 5235–5237.

Teng, Q. and Cross, T.A. (1989) *J. Magn. Reson.*, **85**, 439–447.

Thiel, B.L., Kunkel, D.D. and Viney, C. (1994) *Biopolymers*, **34**, 1089–1097.

Traub, W. (1969) *J. Mol. Biol.*, **43**, 479–485.

Tycko, R. (2001) *Annu. Rev. Phys. Chem.*, **52**, 575–606.

van Beek, J.D., Beaulieu, L., Schafer, H., Demura, M., Asakura, T. and Meier, B.H. (2000) *Nature*, **405**, 1077–1079.

Warner, S.B., Polk, M. and Jacob, K. (1999) *J. Macromol. Sci., Rev. Macromol. Chem. Phys.*, **C39**, 643–653.

Winkler, S. and Kaplan, D.L. (2000) *Rev. Mol.Biotech.*, **74**, 85–93.